DOI: https://doi.org/10.53350/pjmhs22163581

ORIGINAL ARTICLE

Eco-Friendly Synthesis, Antibacterial Activity, and Photocatalytic Performance of Zno Nanoparticles Synthesized via Leaves Extract of Paraserianthes Lophantha

KARRAR HAZIM[1], ZAID HAMZA[2], LIDIA MOHAMED[3], FARIS J. ALYASIRI[4]
[1]*Pharmacy Department, Al-Mustaqbal University College, 51001 Hillah, Babil, Iraq*
[2]*Al-Qadisiyah University College of Pharmacy*
[3]*Al-Zahrawi University College/ Depar/tment of Medical lab-technology*
[4]*Islamic Azad university science and research branch*
Corresponding author: Karrar hazim, Email: karar.hazim@mustaqbal-college.edu.iq

ABSTRACT

This study included the synthesis in environmentally friendly nanotechnologies using the leaf extract of the plant Paraserianthes lophantha. This eco-friendly method is safe and non-toxic or harmful to the environment. The method is economical, easy to operate, and highly efficient, and the properties of the resulting compounds can be controlled, in this way the ZnO compound can be controlled with the same plant extract and by the reaction. The research also included the result and study of the properties of these nanoparticles through various techniques including Field emission-scanning electron microscopic (FE-SEM) X-ray diffraction XRD. atomic force microscopy(AFM).Transmission electron microscopic studies (TEM). Also, the analysis of ZnO NPs was investigated by EDX-mapping and confirmed the existence and efficient degradation of Zn, O in the composite. The efficacy study of the prepared compound using bacteria was used. The activity of ZnO NPs and their effect on antibacterial was studied using two different types of bacteria, Gram negative E. Coli and Gram positive S.aureus e. Also, the photocatalytic ability of ZnO NPs was identified through the photodegradation process of the dyes, as the rhodamine B dye was degraded, and the rate of degradation was 83%. The effect of the amount of the catalyst was studied and quantities (0.2,0.4,0.6,0.8,1, 1.2,1.4,1.6g/L) and the best weight was 1gm and the dye concentration was 10ppm. receivers for electrons as well as those electrons and free holes are working on water and oxygen conversion to ·OH radical with very powerful oxidation.

Keywords: ZnO NPs; photocatalytic degradation; anti-bacterial activity; Paraserianthes lophantha

INTRODUCTION

Environmental pollution is one of the main problems of the world, which includes soil pollution, and air pollution. This problem has increased in recent years due to increased population density, and many factories, so the development of this problem is to be prevented by quality environmental monitoring and evaluation[1] [2] One of the most important ways of monitoring the biological method that includes evaluation many plants, trees, fish as well as bacteria and viruses as indicators in environmental quality control. Waste is one of the most important pollutants that affect the plants, which leads to changes in the quality of the environment, soil and air that affect vegetable and animal life and living organisms[3] [4] . Pollution with heavy metals from the most affected species such as chromium and arsenic ions are carcinogenic materials and absorbs by the digestive system of humans through the skin[5] . The problem of water pollution is one of the main problems at present, due to the increase of organic and inorganic chemical pollutants used in industrial activities, that include toxic metals, dyes, organic pollutants, waste sites and mining operations, the most dangerous to sewage pollution, as these pollutants lead to change physical properties and increase the amount of impurities in water[6, 7]. Nanomaterials feature a wide range of applications used to handle environmental pollution, especially water pollution[8, 9]. Nanoparticles and oxides of some metals constitute effective adsorbents with high efficiency in the treatment of environmental pollution [10] Active carbon, silica, and graphene oxide were used, which has proved to be highly efficient due to its unique two-dimensional nature represented by the presence of functional groups and has a large surface area [11]. The removal of pollutants in non-living biomass is when by alternative and innovative therapeutic technologies, which has gained important credibility due to good performance and low cost[12]. Consideration in environmentally friendly and plant systems, where this method is low-cost and non-harmless, less contaminated and environmental pollution and can be expanded and therefore it is likely to be different from various chemicals [13, 14] .The synthesis of nanoparticles from the green plant is in stages, the first step is the activation stage of metal ions from their salty materials, As for the second stage, it is the stage of synthesis of nanoparticles with the maximum possible activity and the morphology is covered by plant metabolites[15, 16] , ZnO crystallizes in two primary forms: hexa (wurtzite) and cubic zinc blende. It is one of the most important nanomaterials that has been intensively investigated for decades.Zinc oxide nanoparticles are a semiconductor compound with a large energy gap (3.37) electron-volt[17]. In recent years, the literature has reported on many routine synthetic procedures for generating ZnO NPs.These approaches, on the other hand, have several drawbacks, such as high energy consumption, high cost, and the possibility of containing hazardous compounds or dangerous physical therapies[18].There has been a worldwide trend in recent years toward more ecologically friendly nanocatalyst manufacturing processes.Plant extracts, bacteria, fungi, and algae have all been used to biosynthesize ZnO NPs in a variety of ways.Different plant extracts, such as roots, flowers, leaves, stems, seeds, and fruits, have been reported to be used to produce[19]. ZnO NPs.X-ray diffraction (XRD), UV–vis diffuse reflectance spectroscopy (DRS), scanning electron microscopy (FE-SEM), energy-dispersive X-ray spectroscopy (EDX), transmission electron microscopy (TEM), and atomic force microscopy (AFM) techniques were used to characterize the nanomaterials as they were fabricated. .

Preparing the plant extract: A 10 g of fresh leaves of Paraserianthes lophantha are washed with deionized water (DIW) to remove dust and under normal conditions, and then ground using an electric grinder to a very fine powder. and immersed into 100 mL of (DIW), The solution is heated for 30 minutes at 80 °C to obtain the plant extract, then the extract was filtered to remove fine suspended particles, Afterwards, the clear extract was stored at 4 0C to be used in the biosynthesis of ZnO NPs.

Biosynthesis Zinc oxide nanoparticles: A 0. 5 g Zn $(NO_3)_2.6H_2O$ was dissolved into 50 mL of aqueous Sesbania grandiflora extract, followed by continuous magnetic stirring at 80 ^{0}C for about 4 hours for reduction into Zn^{+2} ions. Then, the solution was covered with a dense aluminium foil to avoid any photo interactions and then was left at ambient temperature for 24 hrs. The reaction mixture was centrifuged at 6000 rpm for 20 min. The obtained brown coloured precipitate was repeatedly washed with DIW and ethanol to remove any adsorptive impurities and dried at 80 ^{0}C for 4 hours to produce a pale white solid. The Reduction of zinc nitrate to zinc ions was confirmed by changing the colour from yellow to white. White solid achieved is an indication of ZnO Nps synthesis. The obtained solid was then calcined at 500 °C for 4 hours.

Photocatalytic degradation of RhB dye: Photocatalytic degradation of Rh. B dye, a solution containing ZnO NPS and dye was magnetically stirred for 180 minutes in darkness to achieve the adsorption-desorption equilibrium of dye molecules on the ZnO surface. The photoreactor was equipped with a 200 W Xenon lamp as a visible light source, and a temperature controller. The lamp was centred in the middle of the rector about 10 cm above the reaction mixture. Firstly, 50 mL of 10 ppm of Rh. B was placed in a beaker and a defined amount of photocatalyst was suspended into the dye solution and ultrasonically treated for 15 minutes, then subjected to continuous stirring for 180 minutes in the dark to achieve the adsorption/desorption equilibrium of dye molecules on the surface of the catalyst. In each run, the lamp was turned on to warm up to 5 minutes before irradiation of dye solution. After each run, 5 mL of reaction mixtures were taken at a different time interval and the ZnO was separated by centrifugation at 6000 rpm for 20 minutes. The photodegradation efficiency of Rh. B was calculated by measuring the absorbance at 553 nm corresponding to the maximum absorption wavelength of Rh.B. The photocatalytic degradation efficiency (%) of the ZnO samples for Rh. B dye was calculated using the following equation.

$$\mathrm{PDE\%} = \frac{A_0 - A}{A} \times 100\% \qquad (1)$$

Where A_0 and A represent the absorbance of RhB at zero and at the time (t), respectively. Various operational parameters which influence the degradation efficiency such as catalyst dosage (0.2– 1.8 g/L), and initial dye concentration (10 ppm),

Result and discussion:

X-ray diffraction :XRD analysis determined the phase presence in synthesized nanomaterials. Fig. 1 shows the X-ray pattern of ZnO NPs which are calcined at 500C° . The diffraction of ZnO NPs as the precursor. XRD results indicate the formation of pure hexagonal wurtzite phase and there is no impurities are present. The XRD pattern exhibits the Miller index of (100) , (002) , (101) , (102) , (110) ,(103) , (200) ,(112), (201), (004). In ZnO materials, the main peak intensity is very high, which indicates good crystalline formation. The narrow peaks angles at 2θ are31.0253 °34.4682, °,36.3908 ° .Table 1 shows the crystallite size calculated by using the Debye Scherer equation[20]:

D=K λ/β cos Θ (2)

Table 1: Data of XRD pattern for the synthesized ZnO NPs

No.	Pos. [°2Th.]	FWHM	d-spacing [Å]	Lattice Strain	Average Size (nm)
1	31.0253	0.3327	2.49218	0.0063	
2	34.4682	0.3142	2.48270	0.0040	
3	36.3908	0.2478	2.37199	0.0036	
4	38.6622	0.2016	2.36737	0.0020	
5	47.9731	0.3969	1.82396	0.0042	35.203
6	56.5288	0.3928	1.59087	0.0034	
7	63.1890	0.4391	1.40372	0.0033	
8	68.2747	0.3898 4	1.39925	0.0023	
9	69.1833	0.1799	1.31491	0.0012	
10	70.3015	0.1900	1.32466	0.0006	

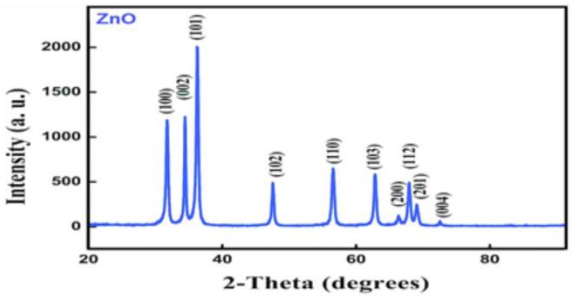

Fig 1: XRD patterns of synthesized ZnO NPs.

Where D is crystal size, K is constant, λ is the wavelength, β is peak width (FWHM), and Θ is diffraction angle [21, 22]

XRD patterns clearly indicate an increase in high-temperature crystals. Increase the volume of pendons (30.03-35.14 nm) upon arrival at the college temperature of 500 ° C.

FESEM Analysis: The FE-- SEM technique is commonly used to determine surface morphology. The FESEM image shown in Figure.2 indicates the formation of ZnO NPs with hexagonal wurtzite structure. All FE-SEM images show some agglomeration of particles [23, 24]

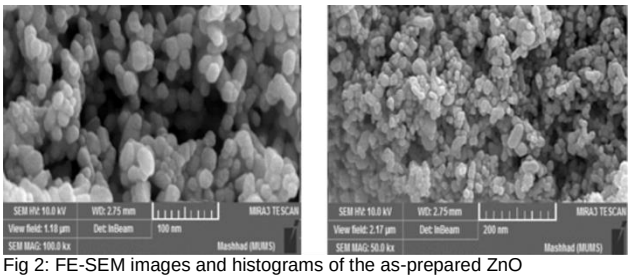

Fig 2: FE-SEM images and histograms of the as-prepared ZnO

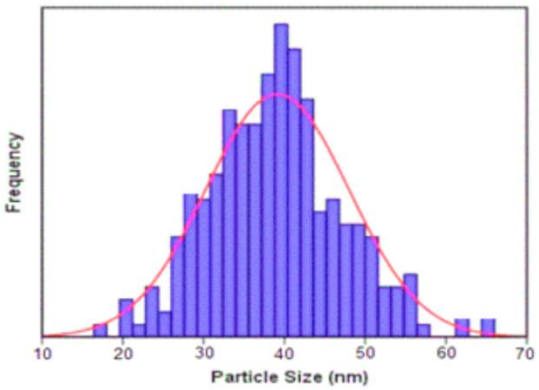

Fig 3:

Transmission Electron Microscopy (TEM): The transmission electron microscope (TEM) is used to study the crystal structure, surface structure, shape, size and distribution of crystals. Figure (4) shows the TEM image with two magnifications of the prepared zinc oxide particles under study using the transmission electron microscope. The high magnification power of the TEM image shows more details about the shape of the particles of the prepared samples, which is between spherical and almost hexagonal in relation to the prepared zinc oxide particles. Here is an ultrasound effect in the formation of zinc oxide particles, and that ultrasound is responsible for reducing the volume of molecules, and the average size of nanoparticles range between 20-100 nanometers, and these results are compatible with former studies [26 ,25] as shown in Figure (4).

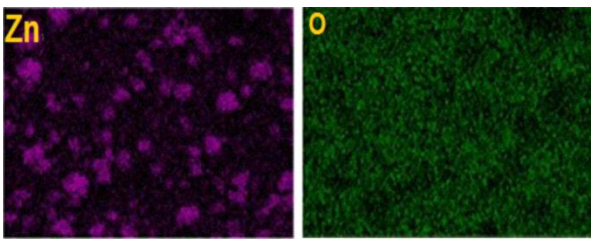

Fig 4: TEM analysis ZnO NPs

AFM analysis : The external morphology and surface characteristics were studied of ZnO NPs using the AFM

technique. This technique was used to know the information of the surfaces, the distribution and homogeneity of the particles and the average size of particle size of syntheaiaed material . AFM analysis provides information about thickness, surface roughness, surface skewness, and surface kurtosis. As can be seen from Figure5, the grain shapes and sizes of ZnO NPs are heterogeneous, and the surface seem to be dense and nearly smooth. As Table 2 shows, the enhanced roughness of the surface by temperature is supported by the observed negative values of skewness, which means the number of surface valleys is higher than peaks [27]. Skewness is a measure of the asymmetry of the probability distribution. Negative skewness represents an advantage of valleys, i.e valleys more than peaks. In addition, kurtosis parameter is a statistical measure used to describe the flatness of the height distribution. For spiky surfaces, Sku >3; for bumpy surfaces, Sku <3; perfectly random surfaces have kurtosis of 3 [28].Figures (a), (b), (c) showed the ratio of the diameter of the ZnO NPs grains and their distribution according to the size, as the distribution of the particles ranged between (45-95 nm) and it was found that the average diameter of the zinc oxide nanoparticles D AVg = 74.82 nm. Figure (a) shows three dimensions X, Y, Z, where the height represents Z = 24.38 nm, and this shows that the zinc oxide nanoparticles are within the range of nanometer dimensions. Figures (b) and (c) show the dense row of nanometric ZnO NPs, as well as the distance between the nanometric particles of zinc oxide, which is equal to 24.38 nm. These figures show the ratio of the average diameter of the zinc oxide grains, as well as their distribution according to that size, we will notice a large increase in the surface area and this means that the size of the particles is smaller ,Where the average roughness (Ra) is 3.13 and the root mean square roughness (Rq) is 3.37, Rku is used to measure the sharpness of the surface if the Rku is equal to 1.53 and the surface is Platkurtic and the thickness of the layer is Thickness 12.49 [25, 29, 30]

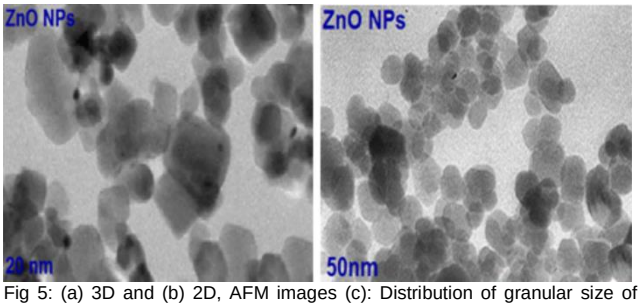

Fig 5: (a) 3D and (b) 2D, AFM images (c): Distribution of granular size of synthesised ZnO NPs.

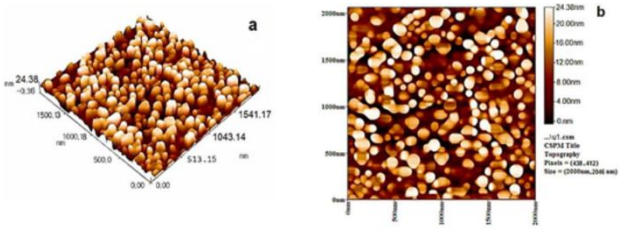

Fig 6: EDX of ZnO NPs

Energy-dispersine x-ray spectroscope (EDX): Figure (6) of the EDX analyzes that were adopted to know the percentage of elements in the show of the ZnO sample .The presence of both elements of zinc and oxygen of the nano-zinc oxide manufactured in a green way was proved by EDX analysis, The EDX results confirmed the presence of very pure ZnO NPS. The atomic ratio between zinc and oxygen is one of the indicators that confirm the formation of ZnO NPS, The oxygen ratio in ZnO samples is 76.79-95.82 and Znic ratio zinc is 4.18 -23.21 which confirms that the synthesized ZnO NPs ,and this is consistent with previous studies[31].

Effect of the amount of photocatalyst : Aseries of the experiments that were conducted to determine the best amount of the catalyst, showed that the amount in which the catalyst had the best performance was 1g/L, where the quantities were tested 0.2g, 0.4g, 0.6g, 0.8g, 1g, 1.2g, 1.4, 1,8 g)), it was found that the efficiency of the catalyst increases with the increase in the amount of the catalyst until a specific amount is reached, after which the efficiency of the catalyst begins to decrease with the increase of the catalyst, as shown in Figure (7), which shows the effect of the amount of the catalyst on the amount of photodegradation efficiency.[32]

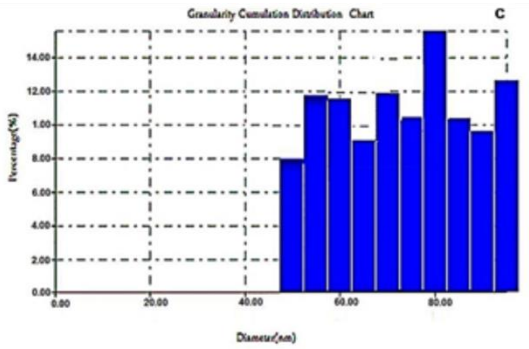

Fig 7: Effect of the amount of photocatalyst on the photodegradation efficiency process (dye concentration 10ppm, temperature 30°C, irradiation time 180minutes[33].

Antibacterial Assay : To study the biological activity of the prepared compounds, two types of bacteria were used, the first bacteria is (Escherichia coli) negative of the chromium dye and the second bacteria is (Staphylococcus aureus), which is positive of the chromium dye. The results showed that the antibacterial activity of zinc oxide E. coli, S. aureus and at two different concentrations /(0.001,0.0005 g/mL) and the results were different, when zinc oxide showed good resistance against both bacteria by disrupting and tearing bacterial membranes. These activities depend on the type of nanomaterials and on the type of bacteria. In addition, there are several factors that can damage or kill bacteria[35,36] including the phenomenon of oxidative stress, genomic and plasmid DNA factors and degradation factors, and it was noted that the number of colonies of E. Coli bacteria is less than the number of colonies of S. aureus bacteria. As in the following figure [37,38].

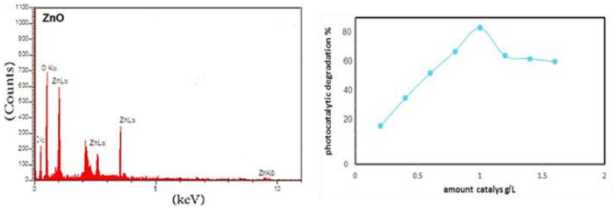

Fig 8: represents the effect of ZnO NPs on E.ColiS bacteria and bacteria S. aureus

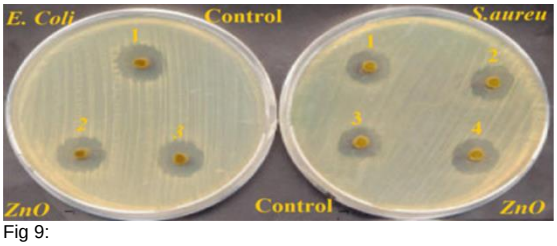

Fig 9:

Mechanisms of the antibacterial activity: The potential toxicity mechanism of ZnO NPS is consistent with the interaction of the ZnO particle with the cell wall, which resulted in a loss of bacterial integrity. The toxicological effect of ZnO NPS against E. coli was studied. The results showed that the bacteria cells were damaged, resulting in the purchase being registered in the membrane; Therefore, there was an increase in membrane permeability, which leads to the accumulation of ZnO NPS in the bacterial cell membrane as well as the internalization of NPS. After contacting ZnO with NPS, the cells contain holes in the membrane. the toxicity of ZnO NPS does not always depend on its uptake into the bacterial cell. ZnO NPS can cause changes in the environment near the bacteria, i.e. ROS production or increased solubility of ZnO NPS, which can induce cellular damage.Suggested

1 ZnO NPs release Zn^{2+} ions, which can be internalised into the bacterial cell and disrupt the enzymatic system.

2 Reactive oxygen species generation (resulting in the breakdown of biological components such as DNA, proteins, and lipids): O_2^- and HO_2^- (do not penetrate the membrane, but direct contact causes damage) and H_2O_2 (do not penetrate the membrane, but direct contact causes damage) (internalised) .

3 Internalization and direct interaction within the bacteria can cause harm such as cellular integrity loss.

Mechanism for photodegradation: photodegradation , charge carrier separation, migration, and surface redox reduction reactions are the main processes in the photocatalytic process . The formation of electron-hole pairs occurs as visible light is emitted on the ZnO catalyst.In the valence band, holes oxidize absorbed hydroxide ions (OH^-) to hydroxyl radicals ($^{\cdot}OH$) , whereas electrons in the conduction band convert O_2 adsorbed onto zinc binding sites to create surfacebound superoxide radicals ($^{\cdot}O_2^-$) Dyes are degraded by these extremely reactive radicals into innocuous species like CO_2 and H_2O.

$ZnO + hv \rightarrow ZnO\ (\ e_{CB}^- + h_{VB}^+)$3

$O_2 + e_{CB}^- \rightarrow {\cdot}O_2^-$ 4

$OH_s^- + h_{VB}^+ \rightarrow {}^{\bullet}OH$5

${}^{\bullet}O_2^- + RhB \rightarrow RhB$ degradation 6

${}^{\bullet}OH + RhB \rightarrow RhB$ degradation7

$RhB + h_{VB}^+ \rightarrow RhB$ degradation 8

CONCLUSIONS

A simple green technique was used to successfully synthesize ZnO NPs.XRD, FE-SEM, TEM, EDX, and AFM techniques were used to examine the structural, morphological, optical, elemental, topographical, and chemical aspects of as-synthesised nanomaterials.With increasing period irradiation, increased photocatalyst loading up to 1.0 g/L, and lowered initial dye concentration, the photodegradation efficiency of RhB dye rose in general.In addition, radical scavenging tests in the photocatalytic system demonstrated that ZnO maintains excellent photocatalytic activity, with hydroxyl radicals and positive holes as the major reactive species.The effectiveness of photocatalysis was 83 %.

REFERENCES

1. Li, K., et al., Sustainable application of ZIF-8 for heavy-metal removal in aqueous solutions. Sustainability, 2021. 13(2): p. 984.
2. Pesce, R., et al., Innovative Magnetic Aggregates for the Removal of Transition Metals from Industrial Wastewater. Minerals, 2021. 11(6): p. 643.
3. Singh, D.K. and M.K. Mondal, Nanoadsorbent: An alternative to conventional adsorbent for water remediation, in Hazardous Waste Management. 2022, Elsevier. p. 397-420.
4. Fei, Y. and Y.H. Hu, Design, synthesis, and performance of adsorbents for heavy metal removal from wastewater: a review. Journal of Materials Chemistry A, 2022.
5. Long, X., et al., Removal of Cd (II) from Micro-Polluted Water by Magnetic Core-Shell Fe3O4@ Prussian Blue. Molecules, 2021. 26(9): p. 2497.
6. Yu, J. and Y. Wang, Policies on seawater desalination and water security in China: Evolution, challenges and recommendations for the future. Journal of Cleaner Production, 2022: p. 130415.
7. Renata, O.-P., et al., Remediation of contaminated water with Chromium VI by sorption in surface-activated-nanocellulose. 2021.
8. Alshamsi, H. and B.S. Hussein, Synthesis, characterization and photocatalysis of γ-Fe2 O3 nanoparticles for degradation of Cibacron Brilliant Yellow 3G-P. Asian J. Chem, 2018. 30(2): p. 273-279.
9. Alshamsi, H.A., M.A. Al Bedairy, and S.H. Alwan. Visible light assisted photocatalytic degradation of Rhodamine B dye on CdSe-ZnO nanocomposite: Characterization and kinetic studies. in IOP Conference Series: Earth and Environmental Science. 2021. IOP Publishing.
10. Hussain, N., et al., Green synthesis of S-and N-codoped carbon nanospheres and application as adsorbent of Pb (II) from aqueous solution. International Journal of Chemical Engineering, 2020. 2020.
11. Elgarahy, A., et al., A critical review of biosorption of dyes, heavy metals and metalloids from wastewater as an efficient and green process. Cleaner Engineering and Technology, 2021. 4: p. 100209.
12. Waheeb, A.S., et al., Myristica fragrans Shells as Potential Low Cost Bio-Adsorbent for the Efficient Removal of Rose Bengal from Aqueous Solution: Characteristic and Kinetic Study. Indonesian Journal of Chemistry, 2019. 20(5): p. 1152-1162.
13. Goga, M., et al., Biological activity of selected lichens and lichen-based Ag nanoparticles prepared by a green solid-state mechanochemical approach. Materials Science and Engineering: C, 2021. 119: p. 111640.
14. Kaabipour, S. and S. Hemmati, A review on the green and sustainable synthesis of silver nanoparticles and one-dimensional silver nanostructures. Beilstein journal of nanotechnology, 2021. 12(1): p. 102-136.
15. KESKİN, C., et al., Environmentally friendly rapid synthesis of gold nanoparticles from artemisia absinthium plant extract and application of antimicrobial activities. Journal of the Institute of Science and Technology, 2021. 11(1): p. 365-375.
16. Srivastava, S., et al., Biological nanofactories: using living forms for metal nanoparticle synthesis. Mini Reviews in Medicinal Chemistry, 2021. 21(2): p. 245-265.
17. Gudkov, S.V., et al., A mini review of antibacterial properties of ZnO nanoparticles. Front Phys, 2021. 9.
18. Zheng, Y., et al., Green biosynthesis of ZnO nanoparticles by plectranthus amboinicus leaf extract and their application for electrochemical determination of norfloxacin. Inorganic and Nano-Metal Chemistry, 2019. 49(9): p. 277-282.
19. !!! INVALID CITATION !!! {}.
20. Khoso, S., et al., GREEN SYNTHESIS OF ZnO NANOPARTICLES FROM FOENICULUM VULGARE, ITS CHARACTERIZATION AND BIOLOGICAL POTENTIAL AGAINST BACTERIA. Journal of Animal & Plant Sciences, 2022. 32(1): p. 229-237.
21. Chikkanna, M.M., S.E. Neelagund, and K.K. Rajashekarappa, Green synthesis of zinc oxide nanoparticles (ZnO NPs) and their biological activity. SN Applied Sciences, 2019. 1(1): p. 1-10.
22. Sahu, D. and N.R. Panda, Exhibition of Novel Photocatalytic Activity and Photoluminescence Properties with High Inhibition Towards Bacterial Growth by Hydrothermally Grown ZnO Nanorods. Current Nanoscience, 2021. 17(1): p. 162-169.
23. Almehizia, A.A., et al., Facile synthesis and characterization of ZnO nanoparticles for studying their biological activities and photocatalytic degradation properties toward methylene blue dye. Alexandria Engineering Journal, 2022. 61(3): p. 2386-2395.
24. Jan, F.A., et al., Exploring the environmental and potential therapeutic applications of Myrtus communis L. assisted synthesized zinc oxide (ZnO) and iron doped zinc oxide (Fe-ZnO) nanoparticles. Journal of Saudi Chemical Society, 2021. 25(7): p. 101278.
25. Al-Kordy, H.M., S.A. Sabry, and M.E. Mabrouk, Statistical optimization of experimental parameters for extracellular synthesis of zinc oxide nanoparticles by a novel haloalaliphilic Alkalibacillus sp. W7. Scientific reports, 2021. 11(1): p. 1-14.
26. Safardoust-Hojaghan, H., et al., Green synthesis, characterization and antimicrobial activity of carbon quantum dots-decorated ZnO nanoparticles. Ceramics International, 2021. 47(4): p. 5187-5197.
27. Akermi, M., et al., Original polymer P-DSBT nano-composite with ZnO nanoparticles for gas sensor at room temperature. Polymer Bulletin, 2021: p. 1-16.
28. Eyvaraghi, A.M., et al., Experimental and density functional theory computational studies on highly sensitive ethanol gas sensor based on Au-decorated ZnO nanoparticles. Thin Solid Films, 2022. 741: p. 139014.

29. Ou, R., et al., Improved photocatalytic performance of N-doped ZnO/graphene/ZnO sandwich composites. Applied Surface Science, 2022. 577: p. 151856.
30. BEHBOUD, A.B., Development of Nanostructured Metallic Glasses with High Toughness. 2021, Middle East Technical University.
31. Rambabu, K., et al., Green synthesis of zinc oxide nanoparticles using Phoenix dactylifera waste as bioreductant for effective dye degradation and antibacterial performance in wastewater treatment. Journal of hazardous materials, 2021. 402: p. 123560.
32. Wu, S., Y. Lin, and Y.H. Hu, Strategies of tuning catalysts for efficient photodegradation of antibiotics in water environments: A review. Journal of Materials Chemistry A, 2021. 9(5): p. 2592-2611.
33. Zyoud, A.H., et al., ZnO-based catalyst for photodegradation of 2-chlorophenol in aqueous solution under simulated solar light using a continuous flow method. JOM, 2021. 73(1): p. 404-410.
34. da Silva, B.L., et al., Relationship between structure and antimicrobial activity of zinc oxide nanoparticles: An overview. International journal of nanomedicine, 2019. 14: p. 9395.
35. Gupta, M., et al., Effective antimicrobial activity of green ZnO nano particles of Catharanthus roseus. Frontiers in microbiology, 2018: p. 2030.
3 Segets, D., et al., Analysis of optical absorbance spectra for the determination of ZnO nanoparticle size distribution, solubility, and surface energy. ACS nano, 2009. 3(7): p. 1703-1710.
37 Wang, J., et al., Synthesis and characterization of multipod, flower-like, and shuttle-like ZnO frameworks in ionic liquids. Materials Letters, 2005. 59(11): p. 1405-1408.
38 Tyshenko, M.G., Risk management and surveillance of nanomaterials for public health, in Nanoengineering. 2015, Elsevier. p. 285-303.